

Motion Performance Analysis and Control Simulation of Manipulator in Chemical Dangerous Goods Detection

Zhiyan Ma

School of Mechanical Engineering, Baoji University of Arts and Sciences, Baoji 721016, China
 mabian12345678@163.com

Due to the maneuverability and operability of a mobile manipulator, the space of its application is greatly extended, especially the mobile manipulator has a wide application prospect in the hazardous areas such as explosive removal, and hazardous leakage material treatment. This paper makes a kinematic and dynamic analysis of the mobile manipulator system for detecting the leakage of chemical dangerous goods, establishes the dynamic analysis model and carries out the motion simulation, together with the simulation and experimental analysis. The effectiveness and reliability of the designed controller are verified by simulation and experiment, the accurate positioning is realized with the mobile manipulator and the sealing system is used to accomplish the task of sealing the leakage of the dangerous chemicals.

1. Introduction

Development of autonomous mobile manipulator systems for detecting and repairing leaks of chemical dangerous goods in synthetic vessels and pipelines can not only avoid leakage accidents in petrochemical industry, but also repair in the event of a slight leak, eliminating the accident in the bud. It is of great practical significance to change the present situation of dangerous goods leakage detection and repair in petrochemical industry of China (Ata, 2017; Berg, 2000). Because mobile manipulator involves many subjects such as machinery, electronics, wireless communication, computer vision, pattern recognition and intelligent control, it will provide an ideal experimental carrier and platform for further research on mobile robot technology.

2. Structure and Motion Analysis of Mobile Manipulator System

2.1 Representation and homogeneous transformation of rigid body pose

In order to describe the kinematic relationship among each link rod of the manipulator itself, and between the manipulator and the environment, the link rod of the manipulator is studied as a rigid body while ignoring the elastic deformation of the link rod of the manipulator.

The space point P may be represented by its three coordinates with respect to the reference coordinate system:

$$P = p_x \hat{i} + p_y \hat{j} + p_z \hat{k} \quad (1)$$

Where p_x , p_y and p_z are the coordinate representing the point in the reference coordinate system. This representation may also vary slightly: Point p is written in vector form and a scaling factor w is added, then point P is represented as

$$P = [x \quad y \quad z \quad w]^T \quad (2)$$

Where $p_x = x * w$, $p_y = y * w$, $p_z = z * w$. The variable w can be arbitrary number, if $w = 1$, the size of each component remains unchanged;

If $w = 0$, x, y and z are infinite, $P = [p_x \quad p_y \quad p_z]^T$ represents a vector of infinite length with the direction represented by the vector. Therefore, $w = 1$ is usually taken, and the vector P represents the position of a

point in the reference coordinate system; take $w = 0$, the vector P represents a direction in the reference coordinate system.

The position of the point in the description space can be described by a position vector, and the pose of a rigid body can be described with a coordinate system fixed on the rigid body (Lu et al., 2016). In order to describe the pose of the rigid body, a coordinate system can be fixed on it, and then the fixed coordinate system can be expressed in space. As long as the coordinate system can be represented in space, the pose of the rigid body relative to the fixed reference coordinate system is also known, as shown in Figure 1.

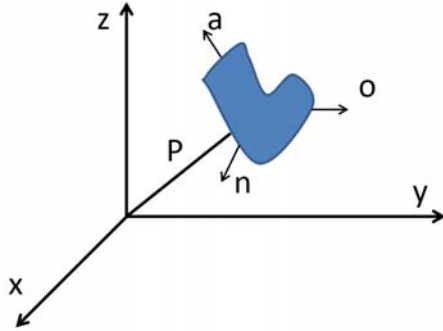


Figure 1: The description of rigid body in the space

If $[p_x \ p_y \ p_z \ 0]^T$ represents the position vector of the origin of the motion coordinate system (current coordinate system) on the rigid body in the reference coordinate system, $[n_x \ n_y \ n_z \ 0]^T$ represents the direction of n axis of the motion coordinate system in the reference coordinate system, $[o_x \ o_y \ 0 \ 0]^T$ represents the direction of the o axis of the motion coordinate system in the reference coordinate system, and $[a_x \ a_y \ a_z \ 0]^T$ represents the direction of the a axis of the motion coordinate system in the reference coordinate system. The pose of the rigid body in the reference coordinate system can thus be expressed as:

$$F_{object} = \begin{bmatrix} n_x & o_x & a_x & p_x \\ n_y & o_y & a_y & p_y \\ n_z & o_z & a_z & p_z \\ 0 & 0 & 0 & 0 \end{bmatrix} \quad (3)$$

Satisfying (1) three vectors are perpendicular to each other; and (2) the length of each unit vector must be 1. This form of matrix is called a homogeneous matrix. And the inverse matrix of such a homogeneous matrix is:

$$\begin{bmatrix} n_x & n_y & n_z & -\bar{p} \cdot \bar{n} \\ o_x & o_y & o_z & -\bar{p} \cdot \bar{o} \\ a_x & a_y & a_z & -\bar{p} \cdot \bar{a} \\ 0 & 0 & 0 & 1 \end{bmatrix} \quad (4)$$

If the rigid body keeps the existing pose unchanged, and only the position in the reference coordinate changes, the position of the new coordinate system with respect to the fixed reference coordinate system can then be obtained using the origin position vector of the original motion coordinate system plus the vector representing the displacement (Turner et al., 2012). In the form of matrix, the representation of the new motion coordinate system can be obtained by left multiplication transformation matrix of the coordinate system. The position of new coordinate system is:

$$\begin{aligned}
 F_{new} = Trans(d_x, d_y, d_z) \times F_{old} &= \begin{bmatrix} 1 & 0 & 0 & d_x \\ 0 & 1 & 0 & d_y \\ 0 & 0 & 1 & d_z \\ 0 & 0 & 0 & 1 \end{bmatrix} \times \begin{bmatrix} n_x & o_x & a_x & p_x \\ n_y & o_y & a_y & p_y \\ n_z & o_z & a_z & p_z \\ 0 & 0 & 0 & 1 \end{bmatrix} \\
 &= \begin{bmatrix} n_x & o_x & a_x & p_x + d_x \\ n_y & o_y & a_y & p_y + d_y \\ n_z & o_z & a_z & p_z + d_z \\ 0 & 0 & 0 & 1 \end{bmatrix}
 \end{aligned} \tag{5}$$

Where d^x , d^y , d^z are the three components of the translation vector d relative to the x , y , and z axes of the reference coordinate system.

Similarly, if the rigid body keeps its existing position unchanged and only changes its pose in the reference coordinate, the representation of the new motion coordinate system can also be obtained by means of left multiplication transformation matrix of the coordinate system (Kanmuri and Moholkar, 2010). For example, where $F_{new} = Rot(x, \theta)$ represents the transformation matrix of the motion coordinate system rotating θ around the x -axis of the reference coordinate system.

2.2 Dynamic analysis of manipulator

The dynamic analysis of a five-degree-of-freedom manipulator mounted on a mobile platform can be obtained by using the aforementioned Recursive Newton-Euler Dynamics Algorithm, but for a multi-degree-of-freedom manipulator, the derivation and calculation of the dynamics equations have become quite complicated. The expression of the forces and moments applied to the joints is more complicated when considering the force exerted by the end effector of the manipulator on the object (Santen, 1995). Here, Lagrangian method, the energy-based dynamics method, is used to describe dynamics equation of the manipulator.

To obtain the Lagrangian function of the manipulator's link rod, first of all, the kinetic energy and potential energy of a point on the i -link rod are analyzed. The derivative θ_i of the matrix iA with respect to its joint variables is:

$$\begin{aligned}
 \frac{\partial A_i}{\partial \theta_i} &= \frac{\partial}{\partial \theta_i} \begin{bmatrix} C_i & -S_i C \alpha_i & S_i S \alpha_i & \alpha_i C_i \\ S_i & C_i C \alpha_i & -C_i S \alpha_i & \alpha_i S_i \\ 0 & S \alpha_i & C \alpha_i & d_i \\ 0 & 0 & 0 & 1 \end{bmatrix} = \begin{bmatrix} -S_i & -C_i C \alpha_i & C_i S \alpha_i & \alpha_i S_i \\ C_i & -S_i C \alpha_i & S_i S \alpha_i & \alpha_i C_i \\ 0 & 0 & 0 & 0 \\ 0 & 0 & 0 & 1 \end{bmatrix} \\
 &= \begin{bmatrix} 0 & -1 & 0 & 0 \\ 1 & 0 & 0 & 0 \\ 0 & 0 & 0 & 0 \\ 0 & 0 & 0 & 0 \end{bmatrix} \times A_i = Q_i \times A_i = Q_\theta \times A_i
 \end{aligned} \tag{6}$$

Using q_i to represent joint variable, the total transformation between the base and the hand of the manipulator is $T_i = A_1 A_2 \dots A_j \dots A_i$. If only one joint variable is derived, then:

$$\begin{aligned}
 U_{ij} &= \frac{\partial T_i}{\partial q_j} = \frac{\partial (A_1 A_2 \dots A_j \dots A_i)}{\partial q_j} = A_1 A_2 \dots Q_j A_j \dots A_i \quad j \leq i \\
 U_{ijk} &= \frac{\partial U_{ij}}{\partial q_k}
 \end{aligned} \tag{7}$$

r_i (vector of 4×1) represents the point of the coordinate system with respect to the i -th link of the robot. Its position in the base coordinate system can be obtained by multiplying the vector to the left by a transformation matrix which represents the coordinate system in which the point is located, so the total kinetic energy of the link i can be expressed as:

$$k_i = \int dk_i = \frac{1}{2} \text{trace} \left[\sum_{p=1}^i \sum_{r=1}^i U_{ip} \left(\int r_i r_i^T dm_i \right) U_{ir}^T \dot{q}_p \dot{q}_r \right] \tag{8}$$

Where $\int r_i r_i^T dm_i$ is the pseudo-inertia matrix J_i of the i -th link rod.

Assuming that the inertia of each driver is $I_{i(act)}$, the total kinetic energy of the link rod of the manipulator is:

$$K = \frac{1}{2} \sum_{i=1}^n \sum_{p=1}^i \sum_{r=1}^i \text{trace}(U_{ip} J_i U_{ir}^T) \dot{q}_p \dot{q}_r + \frac{1}{2} \sum_{i=1}^n I_{i(act)} \dot{q}_i^2 \quad (9)$$

The total potential energy of the link rod of the manipulator is

$$P = \sum_{i=1}^n p_i = \sum_{i=1}^n [-mg(^0 T_i r_i)] \quad (10)$$

Where $g^T = (g^x \ g^y \ g^z \ 0)$ is gravity matrix and r_i is the position coordinate vector of the centroid of link rod in all link rod coordinate systems, $\bar{r}_i = (\bar{x}_i \ \bar{y}_i \ \bar{z}_i \ 1)$.

Lagrangian function of the link rod of the manipulator:

$$L = K - P = \frac{1}{2} \sum_{i=1}^n \sum_{p=1}^i \sum_{r=1}^i \text{trace}(U_{ip} J_i U_{ir}^T) \dot{q}_p \dot{q}_r + \frac{1}{2} \sum_{i=1}^n I_{i(act)} \dot{q}_i^2 - \sum_{i=1}^n [-mg(^0 T_i r_i)] \quad (11)$$

3. Dynamics Simulation of Manipulator

Based on the known joint angle and joint velocity, the cubic spline interpolation function is used to calculate the equation of motion $\theta(t)$ between the acceleration of a joint at the interpolation point of the end effector and the interpolation point of the manipulator.

Let the angle of rotation of a joint θ_i at t_i , θ_f be θ_i and θ_f and the speed be $\dot{\theta}_i, \dot{\theta}_f$, a cubic polynomial can be used to represent the relationship between θ_i and time t :

$$\theta(t) = c_0 + c_1 t + c_2 t^2 + c_3 t^3 \quad (12)$$

This is also true for the function $\theta(tf)$ between two successive interpolation points on the trajectory, taking the time t_i as the initial time 0. At the end of time, and knowing θ_i and $\dot{\theta}_i$ and θ_f and $\dot{\theta}_f$ at the initial time and the end time, which are substituted into the above Formula:

$$\begin{aligned} \theta(0) &= c_0 = \theta_i \\ \theta(tf) &= c_0 + c_1 tf + c_2 t^2 + c_3 t^3 = \theta_f \\ \dot{\theta}(0) &= c_1 = \dot{\theta}_i \\ \dot{\theta}(tf) &= c_1 tf + 2c_2 t^2 + 3c_3 t^3 = \dot{\theta}_f \end{aligned} \quad (13)$$

Since $c_0 = \theta_i, c_1 = \dot{\theta}_i$, then:

$$\begin{aligned} c_2 &= \frac{3(\theta_f - \theta_i) - (2\dot{\theta}_i + \dot{\theta}_f)tf}{t_f^2} \\ c_3 &= \frac{(\dot{\theta}_i + \dot{\theta}_f)tf - 2(\theta_f - \theta_i)}{t_f^2} \end{aligned} \quad (14)$$

The angular velocity and angular acceleration can be obtained from the derivation of the above formula:

$$\begin{aligned} \dot{\theta}(t) &= c_1 + 2c_2 t + 3c_3 t^2 \\ \ddot{\theta}(t) &= 2c_2 + 6c_3 t \end{aligned} \quad (15)$$

It is the angular velocity equation and angular acceleration equation between the interpolation points. In particular, $\ddot{\theta}(0) = 2c_2, \ddot{\theta}(tf) = 2c_2 + 6c_3 tf$ is common acceleration values for two adjacent interpolation points on a trajectory (Yamamoto et al., 2012). Thus, the angular acceleration value required in the process of calculating the torque required for the joint and the equation of the motion of each joint between the interpolation points have been obtained.

The dynamic model is simulated by using the simulation function module of ADAMS. Figure 2 is the dynamic model of the manipulator prototype, with EndTime as 30.0 seconds and Step Size as 0.1.

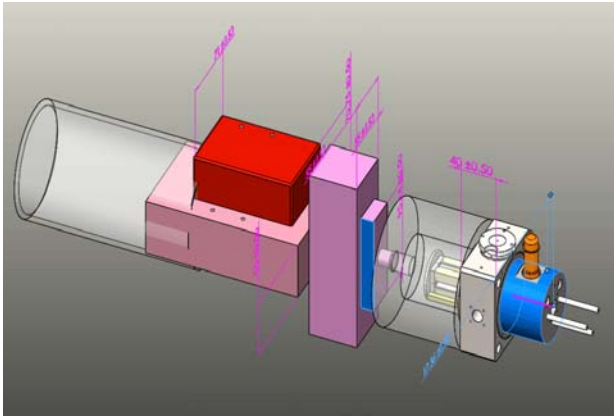


Figure 2: The dynamics model of virtual proto type of manipulator in ADAMS

A driving function (Motion) is defined for each joint (rotating pair):

Motion 1:

step(time,0.0,0.0,30.0,360d)

Motion 2:

step (time,0.0,3.0, -90d) + step(time,9.0,0,12.0,120d) + step (time,27.0,0,30.0, -30d)

Motion 3:

Step (time,3.0,0,6.0, -135d) + step(time,12.0,0,15.0,270d) + step (time,24.0,0,27.0, -135d)

Motion 4:

step(time,18.0,0.0,21.0,360d)

Motion 5:

Step (time,6.0,0,9.0, -90d) + step(time,15.0,0,18.0,180d) + step (time,21.0,0,24.0, -90d)

After the driving function is defined, the prototype of the manipulator needs to be loaded, and the maximum load of the manipulator is 5 kg under actual working conditions. The relationship between the torque of joints 1, 2, 3, 4, and 5 and the pose of the prototype is shown in Figure 3. These figures directly show the change of torque at the five rotating joints when the pose of the manipulator prototype is changed in the simulation process.

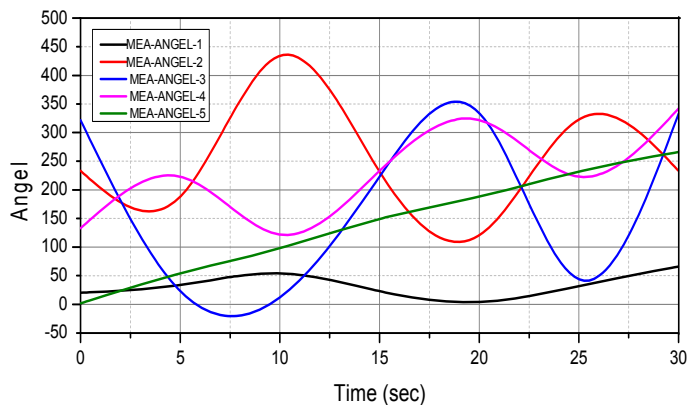


Figure 3: The relationship between torque on joint 1,2,3,4,5 and angles on main joint

The statistical results of the curves shown include a maximum value, a minimum value, an average value, and the like of the curve data points. The results show that the maximum torque of the manipulator prototype's Joint 1 in the y direction is 677Nmm and the time is 13.6s; then, the pose of the manipulator prototype can be determined from the angle values of each joint at this time point; the maximum torque of the manipulator prototype's Joint 2 in the z direction is 39,960Nmm, which occurs at 2.9 seconds, and the maximum bending moment in the x direction is 14,642Nmm, which occurs at 19.6 seconds; the maximum torque of the manipulator prototype's Joint 3 in the z direction is 21,163 Nmm, which occurs at 2.9 seconds, and the maximum torque in the x direction is 15,545 Nmm, at 12.1 seconds; the maximum bending moment of the

manipulator prototype's Joint 4 in the y direction is 335Nmm, which occurs at 20.0 seconds, and the maximum in the negative direction is 333Nmm, which occurs at 19.0 seconds; the maximum torque of the manipulator prototype's Joint 5 in the z direction is 1,395 Nmm, which occurs at 2.9 seconds, the maximum value in the negative direction is 1,249 Nmm, which occurs at 18.8 seconds and the maximum torque in the x direction is 1,274 Nmm, which occurs at 18.8 seconds, and the maximum value in the negative direction is 1,342 Nmm, which occurs at 10.2 seconds. The simulation results show that the positions of 2.9 seconds, 12 seconds and 20 seconds in the simulation process are more dangerous poses of the manipulator, which reflects the relationship between the peak torque and bending moment of each joint and the pose of the manipulator, providing the reference condition for the motion planning and control of the manipulator.

4. Conclusion

According to the motion planning strategy of mobile manipulator, a simplified dynamic model of mobile manipulator is proposed in this paper, and its dynamic model is established by using Newton-Euler method. The simulation analysis under certain conditions shows the dynamic coupling effect between the mobile carrier and the manipulator, and it's found the greater the acceleration of the mobile carrier is, the greater the influence on the joint load moment of the manipulator is, which will affect the dynamic control and steady state control of the system. The dynamic model of mobile carrier and manipulator subsystem is established, the relationship between joint torque and pose of manipulator is obtained through simulation analysis, and the driving torque of left and right front wheels of mobile platform is controlled. The mobile platform can be moved according to a given trajectory, and at the same time, the direction angle of the mobile platform can be changed.

Reference

- Ata A. A., 2017, Dynamic modelling and numerical simulation of a non-holonomic mobile manipulator, *International Journal of Mechanics & Materials in Design*, 6(3), 209-216.
- Berg A. V. D., Dentener F., Lelieveld J., 2000, Modeling the chemistry of the marine boundary layer: sulphate formation and the role of sea-salt aerosol particles, *Journal of Geophysical Research Atmospheres*, 105(D9), 11671-11698.
- Lu R., Lin C., Turco R., Arakawa A., 2016, Cumulus transport of chemical tracers: 1. cloud-resolving model simulations, *Journal of Geophysical Research Atmospheres*, 105(D8), 10001-10021.
- Turner B. R., Armstrong H. A., Wilson C. R., Makhlof I. M., 2012, High frequency eustatic sea-level changes during the middle to early late ordovician of southern jordan: indirect evidence for a darriwilian ice age in gondwana, *Sedimentary Geology*, 251-252(s 251 - 252), 34-48.
- Yamamoto M., Shimamoto A., Fukuhara T., Tanaka Y., Ishizaka J., 2012, Glycerol dialkyl glycerol tetraethers and tex86 index in sinking particles in the western north pacific, *Organic Geochemistry*, 53(12), 52-62.
- Kanmuri S., Moholkar V. S., 2010, Mechanistic aspects of sonochemical copolymerization of butyl acrylate and methyl methacrylate, *Polymer*, 51(14), 3249-3261.
- Mao X.Q., 2018, Design of New Electrochemical Sensors and Detection Application of Chemical Feedstock Residues, *Chemical Engineering Transactions*, 65, 205-210, DOI: 10.3303/CET1865035
- Santen R. A. V., 1995, Catalysis: closing the molecular and macroscopic sciences gap, *Chemical Engineering Science*, 50(24), 4027-4044.